GFF, 2015
Vol. 137, No. 4, 293–303, http://dx.doi.org/10.1080/11035897.2015.1100213

Article

Aerial LiDAR analysis in geomorphological mapping and geochronological determination of surficial deposits in the Sodankylä region, northern Finland

P. SARALA[1*], J. RÄISÄNEN[1], P. JOHANSSON[1] AND K.O. ESKOLA[2]

Sarala, P., Räisänen, J., Johansson, P., & Eskola, K.O., 2015: Aerial LiDAR analysis in geomorphological mapping and geochronological determination of surficial deposits in the Sodankylä region, northern Finland. GFF, Vol. 137, pp. 293–303 doi: http://dx.doi.org/10.1080/11035897.2015.1100213.

Abstract: Geomorphological mapping based on an aerial light detection and ranging (LiDAR)-derived digital elevation model, field observations, ground penetrating radar measurements and test pit surveys was carried out in a glaciogenic environment in Sodankylä, central Finnish Lapland. The mapping area covered about 370 km^2, with the LiDAR data having a pixel size of 2 m × 2 m and vertical resolution 0.3 m. The geomorphology of the area consists of large till-covered hills, ground moraine plains, glaciofluvial sand and gravel deposits composed of esker systems and related delta and outwash formations of the Weichselian cold stages, followed by pro-glacial glaciolacustric and post-glacial lacustric and fluvial sand/silt deposits. Furthermore, large areas in topographical depressions are covered by Holocene mires. The benefits of LiDAR data compared to traditional aerial-photo-based interpretation were in more detailed identification of surface deposits and more precise edging of the morphologies. This reflected more accurately the true ground surface in areas of dense vegetation. As an example, based on the LiDAR mapping it was possible to distinguish several till-covered delta and sandur deposits which based on OSL dating date back to the Early Weichselian stadial (74–89 ka). The results of the mapping project have been collated and published in a Quaternary geological map of the Sodankylä region.

Keywords: Geomorphological mapping, LiDAR; glacial deposits, stratigraphy, geochronology, optical stimulated luminescence, Quaternary, Weichsel, Sodankylä, Finland

[1]*Geological Survey of Finland, P.O. Box 77, FI-96101 Rovaniemi, Finland;*
[2] *Dating Laboratory, University of Helsinki, FI-00014 Helsinki, Finland*

**Corresponding author. Email: pertti.sarala@gtk.fi*
Manuscript received 2 March 2015. Revised manuscript accepted 22 September 2015.

Introduction

In the past, geomorphological mapping was commonly based on interpretation of aerial stereophotographic images supported by field work and stratigraphical observations. However, many details and small surficial features were lost due to the rough resolution and due to vegetation covering the ground and obscuring interpretation. Moreover, in many cases, only greyscale aerial photos were available, limiting surface feature identification.

Light detection and ranging (LiDAR) is a remote sensing technique that measures distance by illuminating a target with a laser and analysing the reflected light. It has numerous applications, and has become an essential tool in high-resolution mapping and remote sensing. Aerial topographical mapping LiDAR equipment generally uses 1064 nm diode-pumped yttrium aluminium garnet lasers (Cracknell & Hayes 2007). The distance between the lasers' transmitter and detector reflected via backscattering is measured, with precise location and height counting based on GPS (Holopainen et al. 2011). High-resolution 3D digital elevation maps generated by airborne LiDAR have led to significant advances in geomorphology and Quaternary mapping. Besides the high accuracy (15 cm/px), another benefit of the method is penetration through forest to the real ground surface (cf. Gil et al. 2013). LiDAR data are now available for many countries. For example, about 300,000 km^2 (ca. 85% of land area) in Finland is already covered by LiDAR data (National Land Survey of Finland; http://www.maanmittauslaitos.fi/en/maps-5).

The high resolution of LiDAR-derived digital elevation models (DEMs) has improved the mapping process by clarifying interpretation of densely forested areas and allowing identification of fine-scale land surface features not originally distinguished in the aerial photos and in the field (Downing et al. 2007; Booth et al. 2009; Howle et al. 2012). Such geomorphologies include low-relief features on top of moraine hills (e.g., flutings and shore deposits), narrow structural lineaments (e.g., postglacial faults) and landslide deposits (e.g., Smith et al. 2014; Sutinen et al. 2014).

LiDAR data are now being used to revise existing geomorphological maps. For example, the U.S. Geological Survey is using LiDAR data due to the high resolution, which has been found to be a great benefit in the mapping process and in distinguishing small morphological features with a host of geomorphological processes (e.g., Haugerud et al. 2003; Burns et al. 2010; Tabor et al. 2011; Howle et al. 2012; Smith & Peterson 2014). Use of LiDAR data in various mapping applications has also been reported for Antarctica (Wilson & Csathó 2007), Canada (Kovanen & Slaymaker 2004), Italy (Cavalli et al. 2008), Scotland (McCormack et al. 2008) and Finland (Nenonen et al. 2010; Palmu & Nenonen 2015).

Geomorphological mapping, particularly in the glaciated areas, commonly includes stratigraphical and geochronological components which help in understanding of processes behind the formation of glaciogenic deposits and their relations to each other. For that purpose, we need soil drilling data and test pit excavations to compile a view of the Quaternary stratigraphy of the study area. Based on identification of separate till units with support of age determination of inter-till layers using modern dating methods such as Optical Stimulated Luminescence (OSL), stratigraphy and geochronology can be combined. New data collected during the mapping program also give a possibility to compare results with older observations made from the area or the reported stratigraphy from the surrounding environs.

The geomorphological mapping described in this paper was carried out in 2013–2014 in the Sodankylä region of northern Finland. The mapping was performed by the Geological Survey of Finland (GTK) with the aims of studying the usability of new LiDAR data in geomorphological interpretation of landform features, instead of conventional aerial photographs, and of revising the old Quaternary map of the area. The mapping project also formed part of GTK's in-house development programme, the aims of which are to examine and renew the mapping procedures used in Quaternary mapping in order to obtain more detailed landform analysis and interpretation and to speed up the mapping procedure. The mapping process is also supported by stratigraphical and geochronological works to better understand the genetic background of the morphologies and deposits but also to collect data to complement a Quaternary geological database from the study area.

Study area and its geology

The study area is located in the centre of Sodankylä municipality (Figs. 1 and 2), in central Finnish Lapland, about 120–150 km north of the Arctic Circle. The basement was formed by the Palaeoproterozoic crystalline bedrock composed of metamorphosed mafic volcanic and sedimentary rocks of the Central Lapland Greenstone Belt (Tyrväinen 1984). The relief is mostly flat or gently undulating, with higher hill areas located in the eastern part of the study area (Fig. 2).

Three previously compiled geomorphological maps on a scale of 1:20,000 are available for the study area (Väisänen et al. 1989; Väisänen & Maunu, 1990, 2004). They cover the centre of the new mapping area, on both sides of the Kitinen river (Fig. 2). The limit for the new mapping area was set based on the extent of LiDAR data published in 2013 and comprises about 370 km^2. The area is challenging for geomorphological mapping because large parts are covered by mires and there are extensive glaciofluvial and fluvial deposits in the north and centre of the area. Only a few field and stratigraphic observations have been made from this area, the most important ones being related to a test pit excavation campaign in the 1970s (Hirvas et al. 1977; Hirvas 1991).

The study area is located close to (on the southern side of) the previous ice divide zone of the Late Weichselian glaciations (Sarala & Ojala 2008; Johansson et al. 2011). Restricted basal erosion rate associated with deposition of new till material is typical for the area. For that reason, the till stratigraphy is commonly composed of more than three till units in Central Lapland, particularly in topographical depressions with thick Quaternary deposits (Hirvas 1991). However, based on earlier stratigraphical data (Johansson 2005), only two separate basal till units can be identified in the study area. The younger (i.e. upper) till was formed during the Late Weichselian glacial phase and the older one has been deposited most probably during the Early or Mid-Weichselian glaciations (Hirvas 1991; Johansson et al. 2011). Above those tills lies surficial till unit representing the last glacier melting phase.

The area deglaciated 10 300 years ago (Johansson & Kujansuu 2005). When the glacier margin retreated downhill in the supra-aquatic area, it dammed meltwaters into proglacial ice lakes. The Moskujärvi ice lake covered low lying areas in the northeastern part of the study area. It grew to a fair size (400 km^2) being in general short-lived. Its water levels lowered as soon as an appropriate outlet channel emerged from the retreating ice margin. Discharging waters often carved remarkable erosional forms in valleys. In the final stage of the last deglaciation, waters of the Ancylus Lake emerged along the Kitinen river valley to the southern part of the area (Johansson 2005). The highest water level was about 190 m (a.s.l.).

Methods

The new mapping process included preliminary interpretation based on the use of LiDAR data and revision of earlier Quaternary maps and reports. The geomorphological interpretation process was supported by the pre-existing soil- and peat-drilling data, geochemical mapping data, stratigraphical observations (mainly from the test pits), bedrock outcrop observations and topographical map databases. Based on the preliminary interpretation, several field observation targets and stratigraphical study points were selected (Fig. 1).

The LiDAR data were obtained during flights by the Finnish National Land Survey in 2009. The density of the LiDAR data was at least 0.5 signal points per square metre, which means a DEMs with 2 m × 2 m horizontal and 0.3 m vertical resolution, respectively. The LiDAR elevation model was visualised by hill shading using NW light with angle 30° or using multidirectional shading as an alternative.

Surficial mapping and soil type observations were carried out in the field with the help of soil observation drill and small

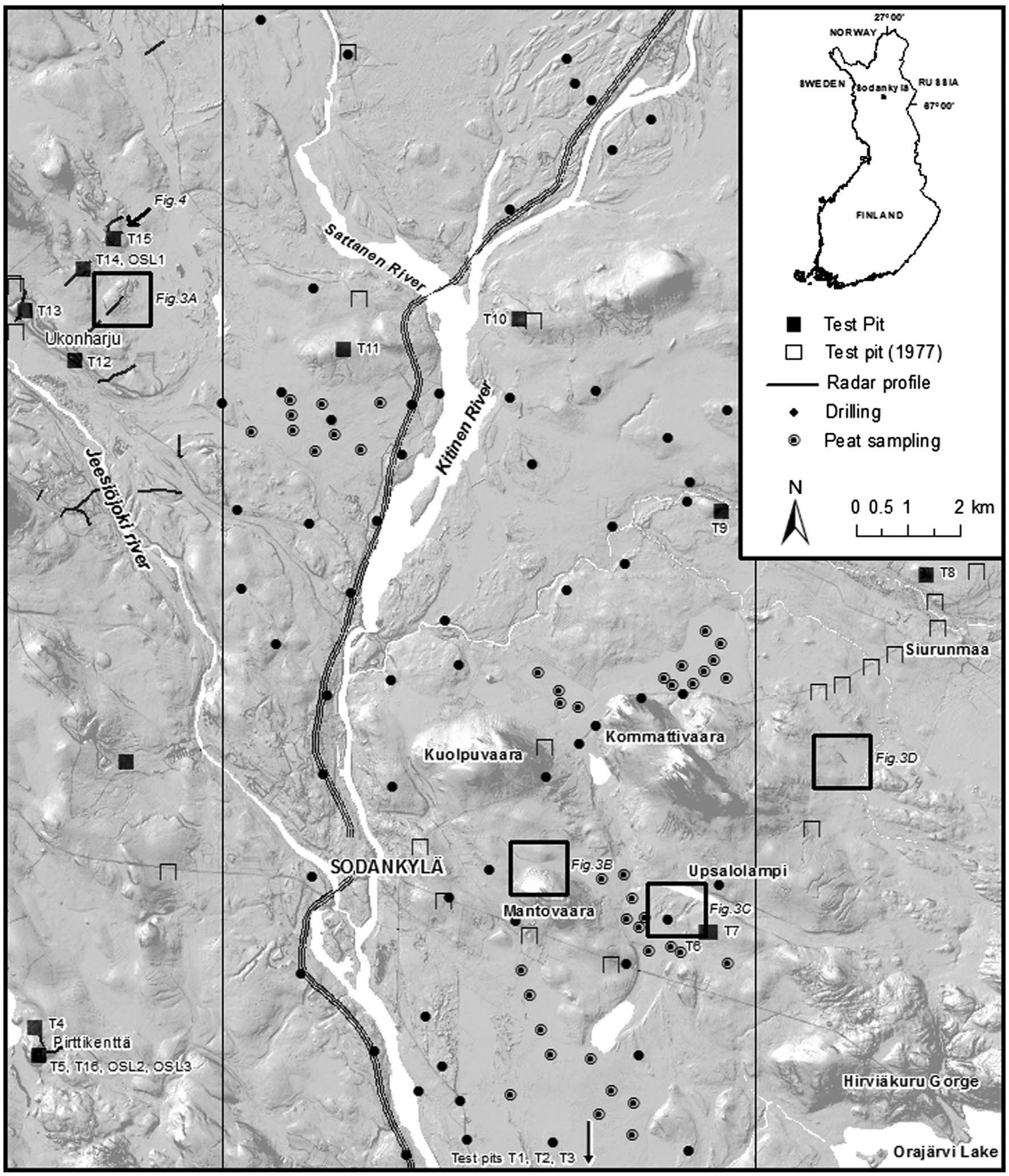

Fig. 1. Hill-shaded LiDAR-derived DEM of the Sodankylä region in central Finnish Lapland and the location of the study area. The sites of new and old test pits, soil drilling and peat survey points and GPR profiles are shown on the map. Test pits 1–3 locate about 5 km south of the mapping area. The large, north–south oriented black rectangle shows the extent of earlier Quaternary maps (see text) in the centre of the study area. Geographic coordinate system: EUREFFIN. Contains data from the National Land Survey of Finland Topographic Database 03/2013.

hand-dug test pits. Observations were stored directly onto a computer in the field using the GTK's ArcMap-based geodatabase application and supported by GPS. Map processing and compilation were performed using ArcMap 10.1 Software.

For the stratigraphical work, both ground-penetrating radar (GPR) and excavator test pits were employed. The GPR system used was 100 MHz cable radar, model Malå (GPR) Rough Terrain Antenna. It is a lightweight apparatus with a small receiving unit and a 7-m long antenna cable. The penetration is up to 30 m depending on soil type and water content or water table height. The total length of the radar survey lines was approximately 10 km and their location is shown in Fig. 1. For radar data processing and interpretation, Geo Doctor 2 Software was used.

Samples for age determinations were collected from the till-covered, stratified sand layers of the two test pits (test pits JPRA-2013-14 and JPRA-2014-16; marked as T15 and T16 in Fig. 1). For sample collection, plastic tubes of diameter 8 cm were used. The sampling tubes were covered by aluminium foil and black plastic to avoid sunlight contamination. Sample preparation

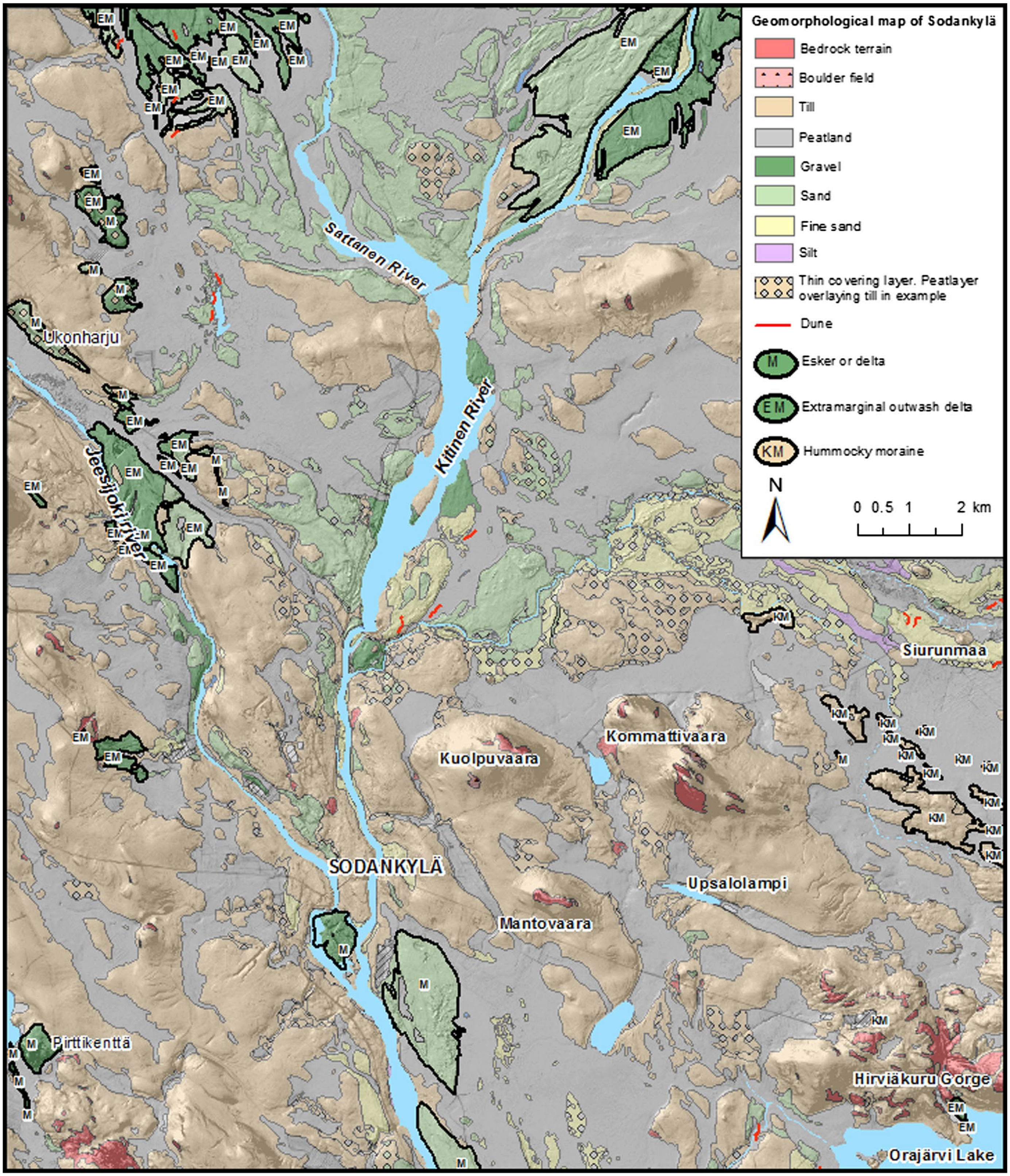

Fig. 2. Geomorphological map of the Sodankylä region in central Finnish Lapland. The hill-shaded LiDAR-derived DEM is in the background. Geographic coordinate system: EUREFFIN. Contains data from the National Land Survey of Finland Topographic Database 03/2013.

and OSL measurements were carried out at the Helsinki University, the Laboratory of Chronology, Finland (3 samples; Hel-TL04289–Hel-TL04291). Quartz equivalent doses were estimated using a post-IR blue Single Aliquot Regenerated dose protocol (Murray & Wintle 2000, 2003). Dose rates were derived from high-resolution gamma spectrometry (Murray et al. 1987), assuming that

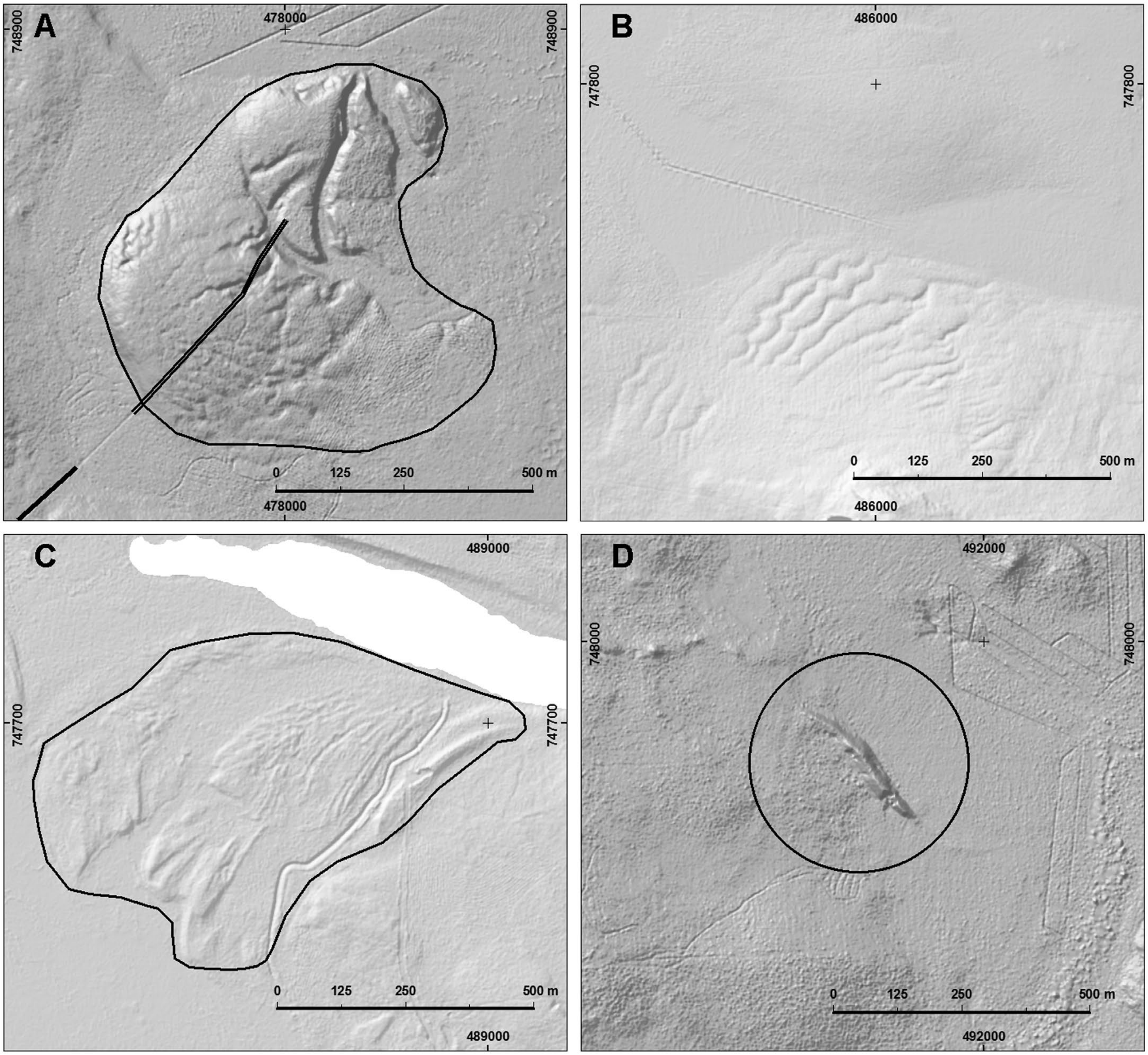

Fig. 3. **A.** Till-covered, stratified sand deposit interpreted as a delta formation after soil drilling observations, GPR profile marked as double line (multidirectional shading); **B**. lateral drainage channels on the northern slope of Mantovaara hill (hill shading); **C**. outwash delta on the southern side of Upsalonlampi (hill shading); **D**. small esker ridge in the forested mire (multidirectional shading). Geographic coordinate system: EUREFFIN. Contains data from the National Land Survey of Finland Topographic Database 03/2013.

samples were fully saturated with water (water content ~20%) most of their burial time. The water content correlation equation for the gamma dose rates (Aitken 1985) was applied to the rates in a water-saturated situation. Cosmic ray dose rates were calculated following Prescott and Hutton (1994). Detailed descriptions of the protocols used for sample processing, beta and gamma dose rate and OSL measurements at the Helsinki University, the Laboratory of Chronology can be found in e.g., Salonen et al. (2008).

Results

Geomorphology

The surface layer of the study area is composed of glaciogenic deposits, mainly (flat) ground moraine areas or moraine ridges composed of sandy till (Fig. 2). Most of the higher ground is covered by variable thickness of till. Bare bedrock and shallow (<1 m) till areas occur only on higher ground, mostly in the SE and SW part of the area. The bedrock in higher hill areas is commonly composed of metasedimentary rocks such as quartzite and mica schists. In lower areas, the bedrock is mainly composed of mica schists and volcanic rocks. Structures of bedrock are also well identified in LiDAR data. Especially, schistosity and jointing in quartzite areas to the north of the Orajärvi lake are iden-

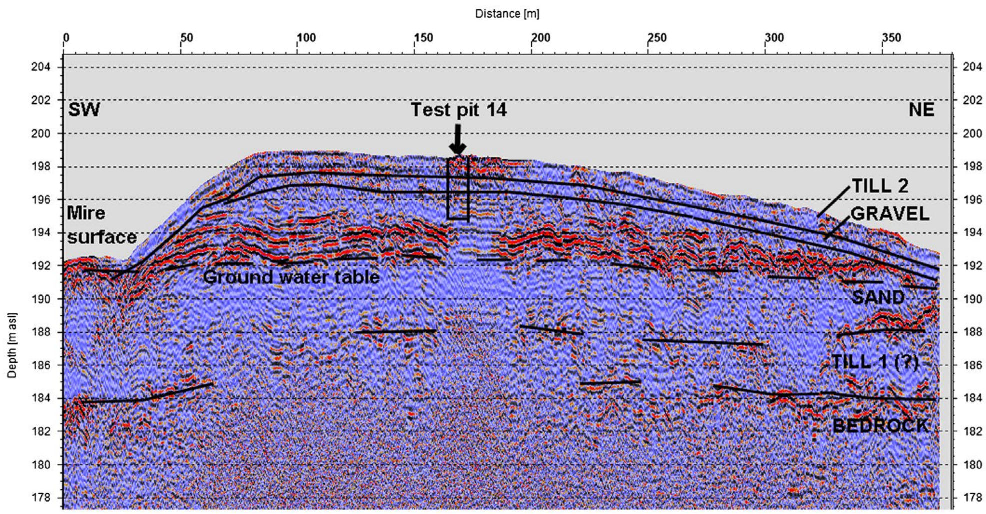

Fig. 4. GPR profile of the till-covered delta formation on the northern side of Ukonharju. Stratigraphical interpretation and the site of test pit JPRA-2014-14 are marked on the profile.

tified easily. In the GTK map of Quaternary deposits, bedrock areas include also areas where the bedrock is covered by a thin (<1 m) surficial sediment layer. There, the structures of bedrock are clearly seen in LiDAR data, and in some areas they are still visible though the soil thickness reaches 2–3 m.

In lowland areas, a basal till layer is generally found, forming moraine topography with a flat or gently undulating surface or as a basement for the peat cover in topographical depressions. The thickness of till layer is typically more than 3 m. The till layer is composed of several till units, the lowest of which, in the deepest depressions, may represent pre-Weichselian glaciations phases (cf. Hirvas 1991). The eastern part of the study area contains a small hummocky moraine field where the thickness of the tills is typically more than 10 m. Glacially streamlined moraine landforms (drumlins and flutings) indicating ice flow direction are not apparent in the area. This is a typical phenomenon of cold-based areas with limited glacial erosion in the central part of glacier and in the ice-divide zone.

Gravel and sand deposits are found occasionally below the surficial till. The shallow relief generally does not give any particular indication of buried sand and gravel deposits. However, based on LiDAR data, it was possible to distinguish surficial features that might reflect till-covered glaciofluvial formations. For example, the network of narrow channels with steep slopes can indicate meltwater erosion through the shallow surficial till (e.g., Fig. 3(A)). Several other similar surface morphologies were examined and the studies revealed quite large till-covered glaciofluvial deposits in the western parts of the study area, which were formerly interpreted as moraine hills composed fully of till. For example, in the Jeesiöjoki river valley and along its northern side, LiDAR data and field observations revealed stratified sand and gravel deposits beneath the till cover (Fig. 2). Based on soil drilling, GPR and test pit observations, the thickness of the surficial till layer is generally 1–2 m in this area. The estimated thickness of the sand and gravel deposits ranged between 2 and 6 m, but they can be markedly thicker in meltwater paleochannels or in deltas. Unfortunately, the relatively high water table restricted identification of deeper structures of stratified sediments or other deposits and the bedrock surface under these from the GPR profiles. A good example of this is provided in Fig. 4, where only the upper till and gravel layers and the upper part of the stratified sands can be seen below the water table.

Fine-grained sediments such as fine sand and silt are also present between surficial peat and till in low-lying areas. Particularly, in the eastern parts, at the Siurunmaa region, larger silt deposits occur under peat cover at topographic depressions. In the northern and western parts, there are some large glaciofluvial or fluvial accumulations, the largest of which form delta-like landforms in the river valleys of Kitinen and Sattanen, but also esker chain and related deltaic sandy deposits in the Jeesiöjoki river valley. Low-lying areas are typically covered by peat (Fig. 2).

Palaeohydrography

LiDAR data are excellent for reconstructing the palaeohydrographical history of the area. On the eastern and southern slopes of the hill Kommattivaara, the northern slope of the hill Mantovaara and the southern slope of the hill Kuolpuvaara, it was possible to identify tens of lateral drainage channels (Fig. 3(B)). These channels formed along the margin of the retreating ice when meltwater eroded the ground. They are almost parallel and slope gently down the hill slopes. Individual channels are few hundreds of metres long. They are 1–3 m deep and open at both ends. They were formed in the margin of the retreating ice sheet by meltwater flowing from the ice and eroding a channel in the slope parallel to the edge of the ice. When the ice became thinner in summer, its surface sank a few metres. The next spring a new channel was again formed below the preceding one. In this way, a series of parallel channels was formed, one below the other. Lateral drainage channels also indicate the gradient of the ice surface, its thinning and outline of the ice margin during the melting phase.

On the eastern slope of the hill Kommattivaara, the channels regularly end at a level of 207 m a.s.l., which was the highest water level of the Moskujärvi ice lake in the northeastern part of the study area (Johansson 2005). The central and western parts of the study area were still covered by the glacier, which prevented meltwater to flow southwards in the Kitinen river valley. The glacier enforced the meltwater streams to flow eastward,

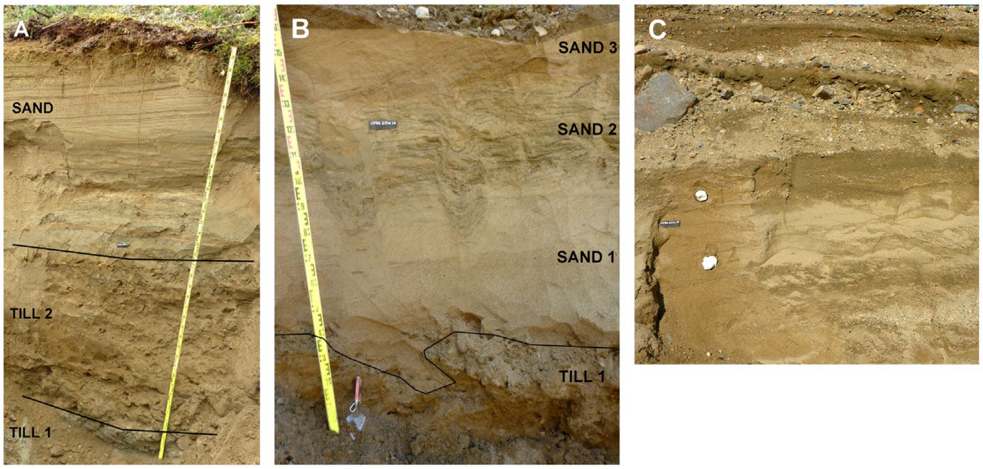

Fig. 5. Interpretation of the stratigraphy **A**. in the test pit JPRA-2014-1 with two till units and glaciofluvial sands on the top; **B**. of the bottom part of till-covered, Early Weichselian deltaic sand deposit in test pit JPRA-2014-13, including till unit 1 on the bottom followed by the planar-bedded sands (SAND 1), ripple-bedded sands (SAND 2) and cross-bedded sands (SAND 3) on top (note load-cast structures in the middle of the photo), OSL sample 1 was taken from the ripple-bedded sand; and **C**. bottom part of the glaciotectonised (faulted), Early-Weichselian sandur deposit with the graded-bedded sand-gravel layers at Pirttikenttä, where the sampling points of OSL2 (upper) and OSL3 are also shown.

Source: Photos P. Sarala

crossing the upland (present-day watershed) between the Kitinen river and Luiro river to the east of the study area.

Later, when the ice margin had retreated to the west, overflow channels from the ice lake turned to the south. Distinct outwash channels with marks of outburst of meltwater masses were formed in the Upsalolampi valley and the Hirviäkuru gorge. It caused a fall of the water level to 200 m (a.s.l.). The outburst caused remarkable erosion on the bottom of the channels. The sediments were carried in suspension to the mouth of the channels where they were deposited. On the southern edge of the Upsalonlampi valley, an outwash delta with shallow gravel deposits and ridge-like formations overlie morainic terrain. Delta formation is easily identified in the LiDAR data (Fig. 3(C)). The youngest spillway of the Moskujärvi ice lake was located on the northern side of Orajärvi lake, at the Hirviäkuru gorge. Its basement at the northern end controlled the height of the ice lake to 195 m (a.s.l.) (Johansson 2005). One of the best ancient shore deposits of that phase is on the northern side of Siurunmaa.

The water body of the Ancylus Lake and its shore phases (below the level of 190 m a.s.l.) have had some effect on the surface of moraine hills during the isostatic land uplift. Boulder fields are better seen on hill tops or slopes, because part of the fine till material has been washed away. In places, there are stratified shore deposits from sand to gravel and washed boulder fields with a thickness from some tens of centimetres to several metres. The surface of sand-covered areas has been commonly been reworked by wind action, forming dunes and dune fields.

When deglaciation continued and the glacier had retreated from the study area to the west, large meltwater streams flowed through the northern and western parts of the study area, causing large areas to be predominantly covered by sand and gravel deposits. For example, in the Sattasjoki river valley (NW part of the study area), extra-marginal outwash gravels formed large deposits connected to similar deposits in the Kitinen river valley (Räisänen 2014). In the northern and central parts, these turned into sandy delta deposits following the highest shoreline of the Ancylus Lake. In the mid-western parts, the Jeesiöjoki river valley acted as an outwash channel to the eastward water streams from the collapsing Ounasjoki ice lake in western Lapland (cf. Johansson 2005). Some gravel deposits still persist as remnants of that outwash. In the middle of the study area, the outwash channel joined the Kitinen river valley. Furthermore, some outwash gravels were deposited in the mouth of narrow ice margin paleochannels. In places, small NW–SE-orientated esker ridges can be found (Fig. 3(D)) indicating the retreat direction of the ice margin during the last deglaciation.

Fine-grained sediments, mostly fine sand and silt deposits, are common, particularly in the low-lying areas where large mires also occur. In the eastern parts of the area, fine-grained sediments are typical below 205 m a.s.l., as markers of the sedimentation process during the Moskujärvi ice lake phase, before the Ancylus Lake. In the central and southern parts, fine sands and silts were deposited during the Ancylus Lake phase and can be found below 186 m a.s.l.

Fine-grained fluvial sediments were also distinguished on both sides of the Kitinen river. They were deposited as flood sediments in topographical depressions, where dunes composed of silt and sands are common and indicate aeolian activity following deglaciation and in the later post-glacial period. Even small and low dune ridges are well identified in the LiDAR data.

Glacial stratigraphy

Test pit observations revealed the till stratigraphy of the area. The observations agreed with the previously reported (e.g., Johansson 2005) till stratigraphy of two distinct basal till units occurring in the area. The lower till, which is grey or dark grey, relatively compact, and has a silt matrix, represents the older glacier's advance in the study area. There were only a few observations of the lower till in the deepest sections, e.g., in test pit 1 (JPRA-2014-1), where the lowest till unit can be found below upper tills (Fig. 5(A)). The boundary to the upper till is distinct and erosional, and also noticeable due to a clear difference in

Table 1. List of OSL results from the Sodankylä region. Samples were dated in the Helsinki University, the Laboratory of Chronology, Finland. Sample numbers refer to the sampling points cited in text and in Fig. 1. Water content assumed to be 20%.

Helsinki code	Sample code	Site	Depth, m	Dose rate, Gy/ka	Equivalent dose D_e, Gy	Number of estimates (*n*)	Age, ka
Hel-TL04289	OSL1 (JPRA-2014-14.1)	Ukonharju, Sodankylä	3.5	1.94 ± 0.24	173 ± 30	5	89.5 ± 19.5
Hel-TL04290	OSL2 (JPRA-2014-16.1)	Pirttikenttä, Sodankylä	4.6	2.14 ± 0.27	175 ± 9	6	81.7 ± 11.6
Hel-TL04291	OSL3 (JPRA-2014-16.2)	Pirttikenttä, Sodankylä	4.9	1.94 ± 0.25	144 ± 19	6	74.2 ± 14.2

colour. Its texture was mostly massive having only some deformation structures in the upper part (flame structures and shearing) Till fabric analyses indicated ice flow direction (260°–270°) from west to east, which was supported by the striae observation (280°) in test pit 11 (JPRA-2014-11).

The upper till, observed in test pits all around the study area, is brownish grey and has a sandy matrix. A moderate number of partly angular but mostly rounded pebbles and boulders is present. The texture is mostly massive and partly deformed, including structures such as laminae and discontinuing sandy lenses or layers within the till. Faults and other glaciotectonic structures are absent. Pebble orientation is in line with the latest ice flow direction (NW to SE) representing the Late Weichselian glaciation.

In several places, there are stratified sand and gravel deposits between the till beds. These are mostly thin (10–30 cm), heterogeneous and deformed, showing clear indications of glaciotectonised disturbance. In western parts of the study area, thick inter-till stratified sand deposits were observed in several places. These sand deposits include several facies from planar and cross-bedded units to climbing ripple laminae (Fig. 5(B)), reflecting shallow, streaming water conditions, most probably a deltaic environment. The stratified sands are deformed, including faults and load-cast structures (Fig. 5(B)).

Furthermore, in the SW corner of the study area, at Pirttikenttä, there is also a relatively thick stratified sandy/gravelly deposit, of which the upper 6–8 m consists of a coarse gravelly/bouldery gradational, stratified unit with sandy lenses and interlayers. The lower part of the deposit is composed of a compact, stratified, sand-dominated unit. Detailed examination revealed several thin (thickness 10–30 cm) layers of graded bedded gravel–sand sequences (Fig. 5(C)). The whole deposit resembles pro-glacial glaciofluvial deposition, i.e. sandur formation, including a complex of braided meltwater streams and outburst mass flow sediments. In addition, the deposit is strongly faulted, a sign of brittle deformation caused by glaciotectonic overthrust.

In some places, particularly river valleys, stratified sand deposits can be found on top of the upper till. They were deposited as glaciofluvial or glaciolacustric deposits during the last deglaciation (e.g., Fig. 5(A)) or as fluvial/lacustric deposits during the post-glacial river and lake phases. In low-lying areas, this stratigraphy is followed by the fine sand and silt layers of the Ancylus Lake beneath the peat deposits.

Age determinations

Three OSL dating samples were collected from the till-covered deltaic sand deposit in Ukonharju (Hel-TL04289) and from the sands in the lower part of the sandur in Pirttikangas (Hel-TL04290- Hel-TL04291; Fig. 5(C)). Fine sands in Ukonharju were collected from the layer of ripple marked sands (Sand 2 in Fig. 5(B)) indicating a shallow water body with some streaming water and/or wave activity. Sands were deposited during NW–SE-oriented water streaming and were also disturbed (i.e. glaciotectonised) due to pressure of moving glacier. Coarse/medium sand samples in Ukonharju were collected in the middle parts of two separated, about 20 cm thick layers of the graded bedded gravel–sand sequences, which represent two different pulses of melt-water to the meandering stream that formed the sandur deposit. Braided water flow direction ranged from N to NW, but later on sand–gravel layers were glaciotectonised including faults that represent different directions.

Ages from the two sampling sites were found to range from 74 to 89 ka (Table 1). The ages are younger in the sandur deposit on the southern part of the mapping area. Relatively high variation in ages and the location of younger age deeper in the profile indicate the presence of older material in the dated samples, and is a sign of partly incomplete bleaching during the deposition. In the ice marginal conditions, it is not unusual because part of the material is released as slurry from the melting ice to meltwater streams preventing sun light from reaching all the sand material deposited into sandur. The formation of this deposit happened during the deglaciation phase of the late Early Weichselian glaciation, around 80–85 ka, i.e. most probably during the Rederstall Stadial, MIS 5b, but having also an indication of possible sedimentation during the following interstadial stage, MIS 5a.

The sands in the second sampling site are the oldest of the dated materials and revealed a part of the material to have been redeposited. High variation in ages is also indicating the presence of sand particles bleached within a relatively long period. However, a short distance between the sampling locations and a relation between meltwater systems together with constant till cover indicate the formation of both deposits during the same deglaciation phase.

Discussion

LiDAR-based mapping of surficial geomorphology provides a very powerful tool for identifying the variety of surficial deposits and landforms in glaciated, forested terrain. Using high-resolution LiDAR data, it is possible to identify more details on the ground compared with 3D aerial photo interpretation. The benefit is that various surficial landforms that indicate glaciogenic objects and ice flow direction can be mapped in detail (e.g., Webster et al. 2006). Glaciofluvial deposits such as eskers and deltas are also possible to discern and delineate without field examination. Furthermore, till-covered glaciofluvial, stratified deposits were revealed to be common in the central part of glaciated areas, but only distinct esker deposits have been recognised in studies based on conventional mapping methods. Using the LiDAR data, it was possible to identify many types of glaciofluvial deposits and even flat, till-covered delta and sandur areas, as well as marginal and extra-marginal deposits. For example, based on the present observations and interpretations from the Sodankylä region, it seems like till-covered gravel and sand deposits are more widespread than reported in previous mapping. However, further studies are needed to confirm this.

Of the small morphologies, dunes were the most easily recognised from the LiDAR-derived DEMS. In addition, several types of small, previously unknown channels were identified. On many flat moraine hills, the channel network seems to indicate glaciofluvial sand and gravel deposits underlying the shallow (1–2 m) till cover. New observations of sand and gravel deposits help determine the relationship between the broken chain of till-covered glaciofluvial deposits such as eskers and deltas, and thereby understand formation of the glaciomorphology in certain areas.

Laser scanning data permit very detailed identification and mapping of surficial features on dry land and mires. The boundaries of different morphologies, for example the edges of mires, are much easier to distinguish than when only aerial photos are used. Certain geological structures such as small channels, shore deposits and landslides were easily recognised from the ground. For example, marginal channels and outwash gravel ridges were found on the hill slopes and the channel/river valleys.

Development of ice-lakes with their spill way networks are one of the best examples of the applicability of LiDAR data in geomorphological studies (Johansson & Palmu 2013). Patterns of the outwash and meltwater channels and their end points at different elevations are good evidence of the lake surface level changes and the highest water tables. However, based on our experiences in this study, other indicators for lake water levels are not so clear. Only shore deposits can be distinguished because they form long, continuous steps on the hill slopes and ground. The wave-washed zone cannot be identified in the LiDAR data and the shore deposits are only seen as a weak boulder belt in the field. Above the highest shoreline, the top of the hills were preserved under a till cover. In contrast, in low-lying areas fine-grained sediments from the washed deposits were deposited on the bottom of ice lakes. The boundary between till and littoral sediments as well as dunes can be identified clearly in LiDAR data.

Bedrock outcrops and very thin till-covered areas were the most difficult to interpret from the laser scanning data. In the GTK Quaternary geological maps, areas having less than 1 m thick soil cover are marked as bedrock areas. In the LiDAR-derived DEMs, bedrock surface morphology and structures can influence the surficial soil morphology even if the soil depth is 2–3 m. This can lead to false interpretations if complementary field observations are not used. Similarly, large boulders and anthills can be interpreted as bedrock features. Moreover, in the case of deposits that are formed of double or triple overlying shallow soil layers, LiDAR is not providing any benefit in a mapping purpose. LiDAR is also not suitable when looking for the edges of landforms composed of very fine-grained sediments in flat terrain.

Based on the present experience, the greatest benefit of LiDAR is during the final decision-making on recognising morphological objects after preliminary interpretation and field work. Having a great amount of detail usually helps in drawing boundary lines, although sufficient stratigraphical information (soil drillings, GPR data and test pits), especially from key places, is needed to support decision-making. It is fairly clear that when LiDAR is used during geomorphological mapping, the need for field work is diminishing without losing too much quality. This is a great benefit in improving the mapping process and increasing cost-effectiveness.

The age of the till-covered stratified, sand and gravel deposits is quite typical for the area and represents the same Early Weichselian deglaciation phase, most probably the Rederstall Stadial, MIS 5b, and/or maybe the next interstadial stage. That correlates well with recent reports from Sokli (Alexanderson et al. 2008) and Rautuvaara (Lunkka et al. 2015) in central Lapland. New age estimations are based on the OSL method, which have been criticised due to possible sources of errors such as incomplete bleaching, which can lead to an age overestimate, or the stability of water content through the deposits' history (cf. Aitken 1985; Kolstrup 2007; Kolstrup et al. 2007; Fuchs & Owen 2008). For example, the effect of water content variation on the calculated OSL age for each 1% increase in water content is estimated to generate an age increase of ca. 1% (Turney et al. 2008). An opposite situation will make deposits younger, but this speculation does not give any correct answer due to poor knowledge of ground water level variation through the long archive history of the deposits. Anyhow, the OSL ages of the till-covered sediments in the Sodankylä region are largely supported by the number of reports of Early Weichselian deposits in central Lapland and northern Finland (Mäkinen 2005; Helmens, Bos et al. 2007; Alexanderson et al. 2008; Sarala 2012; Lunkka et al. 2015). Furthermore, based on till stratigraphy, commonly occurred inter-till stratified sand and gravel deposits, for example in the Sodankylä region, were interpreted to be Early Weichselian (cf. Hirvas 1991; Johansson et al. 2011).

Large-scale occurrence of the sand and gravel deposits under the Late Weichselian tills indicates weak glacial erosion in the last ice divide zone. There are also many reports of Middle Weichselian inter-till glaciofluvial deposits in central Lapland (Sarala et al. 2005; Helmens, Johansson, et al. 2007; Sarala et al. 2010; Sarala and Eskola, 2011; Salonen et al. in press), but no indication of this could be found from the Sodankylä region in the present study. However, there were signs of some subglacial or glaciofluvial deformation and possible erosion in the upper part of the stratified sediments and in the contact to the upper till. Furthermore, the third till bed representing Middle Weichselian till is missing in the area. This leads to the assumption of loss of some glaciogenic units between the Early Weichselian sediments and the Late Weichselian till. It is possible that meltwater streams were repeatedly directed to the same channels, destroying most of the older sediments.

Conclusions

The applicability of LiDAR-derived DEMs in geomorphological mapping was tested in the Sodankylä region, northern Finland in this study. Older Quaternary maps in the area were based on conventional aerial photo interpretation. The aim in this project was to find out benefits of the use of the new LiDAR-based mapping procedure to estimate the need for field observations and other helpful data-sets in final decision-making on morphological objects or formation boundaries, and to revise the old Quaternary geological maps (1:20,000 scale) for the centre of the new mapping area.

It was a clear and obvious benefit for the whole mapping process that through using the LiDAR data, a huge increase in detail, including small surficial features in densely forested areas, could be obtained without field work. In shallow till areas, an influence of underlying features was apparent in the surficial morphology. This is an advantage in the case of till-covered stratified sand and gravel deposits, but a possible source of false interpretations in the case of bedrock outcrops or very thin soil cover areas. Although the use of LiDAR data in geomorphological mapping will improve the cost-effectiveness and speed up the mapping process, supporting stratigraphical data-sets and e.g., soil thickness observations are still needed.

Based on the LiDAR data, several large till-covered, stratified, glaciofluvial sand and gravel deposits were found, particularly in the western parts of the study area. OSL dating results indicate that these deltaic and sandur formations developed during the Early Weichselian stadial phase (74–89 ka), probably during the Rederstall Stadial, MIS 5b. This indicates that the deglaciation phase of the first Weichselian glacial advance reached the Sodankylä area after a previous warm interglacial period.

Acknowledgements — The authors wish to thank GTK's LiDAR mapping project, led by Dr Jukka-Pekka Palmu, for support during the testing process. GPR measurements and image processing were carried out by Hannu Panttila and Juho Kupila, to whom we express great gratitude. Dr Jakob Heyman and one anonymous reviewer are thanked for constructive comments of the manuscript.

References

Aitken, M.J., 1985: *Thermoluminescence dating*. Academic Press, New York. 351 pp.

Alexanderson, H., Eskola, K.O. & Helmens, K.F., 2008: Optical dating of late Quaternary sediment sequence from Sokli, northern Finland. *Geochronometria 32,* 51–59.

Booth, A.M., Roering, J.J. & Perron, J.T., 2009: Automated landslide mapping using spectral analysis and high-resolution topographic data: Puget Sound lowlands, Washington, and Portland Hills, Oregon. *Geomorphology 109,* 132–147. doi: http://dx.doi.org/10.1016/j.geomorph.2009.02.027.

Burns, W.J., Coe, J.A., Kaya, B.S. & Ma, L., 2010: Analysis of elevation changes detected from multi-temporal LiDAR surveys of forested landslide terrain in western Oregon. *Environmental & Engineering Geoscience XVI,* 315–341.

Cavalli, M., Tarolli, P., Marchi, L. & Fontana, G.D., 2008: The effectiveness of airborne LiDAR data in the recognition of channel-bed morphology. *Catena 73,* 249–260.

Cracknell, A.P. & Hayes, L., 2007: *Introduction to remote sensing*. 2nd ed. Taylor and Francis, London.

Downing, J.B., Konsoer, K.M. & Kite, J.S., 2007: LiDAR based surficial geology mapping in comparison to more traditional methods in the heavily vegetated Appalachian mountains. 2007 GSA Denver Annual Meeting (28–31 October 2007). *Geological Society of America Abstracts with Programs. 39,* 161.

Fuchs, M. & Owen, L.A., 2008: Luminescence dating of glacial and associated sediments: review, recommendations and future directions. *Boreas 37,* 636–659. doi: http://dx.doi.org/10.1111/j.1502-3885.2008.00052.x.

Gil, A.L., Núñez-Casillas, L., Isenburg, M., Benito, A.A., Bello, J.J.R. & Arbelo, M., 2013: A comparison between LiDAR and photogrammetry digital terrain models in a forest area on Tenerife Island. *Canadian Journal of Remote Sensing 39,* 396–409.

Haugerud, R.A., Harding, D.J., Johnson, S.Y., Harless, J.L., Weaver, C.S. & Sherrod, B.L., 2003: High-resolution lidar topography of the Puget Lowland, Washington – a Bonanza for Earth Science. *GSA Today 13,* 4–10.

Helmens, K.F., Bos, J.A.A., Engels, S., Van Meerbeeck, C.J., Bohncke, S.J.P., Renssen, H., Heiri, O., Brooks, S.J., Seppä, H., Birks, H. J.B. & Wohlfarth, B., 2007: Present-day temperatures in northern Scandinavia during the last glaciation. *Geology 35,* 987–990. doi: http://dx.doi.org/10.1130/G23995A.1.

Helmens, K., Johansson, P., Räsänen, M., Alexanderson, H. & Eekola, K., 2007: Ice-free intervals continuing into marine isotope stage 3 at Sokli in the central area of the Fennoscandian glaciations. *Bulletin of the Geological Society of Finland 79,* 17–39.

Hirvas, H., 1991: Pleistocene stratigraphy of finish Lapland. *Geological Survey of Finland, Bulletin 79,* 123 p.

Hirvas, H., Altfan, A., Pulkkinen, E., Puranen, R. & Tynni, R., 1977: Raportti malminetsintää palvelevasta maaperätutkimuksesta Pohjois-Suomessa vuosina 1972–1976. [Summary: a report on glacial drift investigations for ore prospecting purposes on northern Finland 1972–1976.] *Geological Survey of Finland, Report of Investigation 19,* 54 p.

Holopainen, M., Hyyppä, J., Vastaranta, M. & Hyyppä, H., 2011: Laser scanning in forests. *Photogrammetric Journal of Finland* 22, 128–149.

Howle, J.F., Bawden, G.W., Schweickert, R.A., Finkel, R.C., Hunter, L.E., Rose, R.S. & von Twistern, B., 2012: Airborne LiDAR analysis and geochronology of faulted glacial moraines in the Tahoe-Sierra frontal fault zone reveal substantial seismic hazards in the Lake Tahoe region, California-Nevada, USA. *Geological Society of America, Bulletin 124,* 1087–1101. doi: http://dx.doi.org/10.1130/B30598.1.

Johansson, P., 2005: Jääjärvet. *In* P. Johansson & R. Kujansuu (eds.): *Pohjois-Suomen maaperä – Maaperäkarttojen 1:400 000 selitys with Summary: Quaternary deposits of Northern Finland – Explanation to the maps of Quaternary deposits 1:400 000*, 127–149. Geological Survey of Finland, Espoo.

Johansson, P. & Kujansuu, R., 2005: Deglasiaatio. *In* P. Johansson & R. Kujansuu (eds.): *Pohjois-Suomen maaperä – Maaperäkarttojen 1:400 000 selitys with Summary: Quaternary deposits of Northern Finland – explanation to the maps of Quaternary deposits 1:400 000*. 149–157. Geological Survey of Finland, Espoo.

Johansson, P., Lunkka, J.P. & Sarala, P., 2011: Glaciation of Finland. *In* J. Ehlers, P.L. Gibbard & P.D. Hughes (eds.): *Developments in Quaternary science*. Vol. 15, 105–116. Elsevier, Amsterdam.

Johansson, P. & Palmu, J.-P., 2013: LiDAR data and elevation model used to produce information of geological landforms and development of ice lake stages. *In* A. Damusyte & A. Grigiene (eds.): *INQUA Peribaltic Working Group. Abstracts of International Field Symposium*. June 25–30, 38–39. Vilnius-Trakai.

Kolstrup, E., 2007: OSL dating in palaeoenvironmental reconstructions. A discussion from a user's perspective. *Estonian Journal of Earth Sciences 56,* 157–166.

Kolstrup, E., Murray, A. & Possnert, G., 2007: Luminescence and radiocarbon ages from laminated Lateglacial aeolian sediments in western Jutland, Denmark. *Boreas 36,* 314–325.

Kovanen, D.J. & Slaymaker, O., 2004: Relict shoreline and ice flow patterns of the northern Puget Lowland from lidar data and digital terrain modelling. *Geografiska Annaler 86,* 385–400.

Lunkka, J.P., Sarala, P. & Gibbard, P.L., 2015: The Rautuvaara stratotype section, western Finnish Lapland revisited – new age constraints on the sequence indicate complex Scandinavian Ice Sheet history in northern Fennoscandia during the Weichselian Stage. *Boreas* 44, 68–80. doi: http://dx.doi.org/10.1111/bor.12088.

Mäkinen, K., 2005: Dating the Quaternary in SW-Lapland. *Geological Survey of Finland, Special Paper 40,* 67–78.

McCormack, D.C., Irvinga, D.H.B., Brocklehursta, S.H. & Rarit-ya, F., 2008: Glacial geomorphological mapping of Coire Mhic Fhearchair, NW Scotland: the contribution of a high-resolution ground based LiDAR survey. *Journal of Maps 4,* 315–331. doi: http://dx.doi.org/10.4113/jom.2008.1033.

Murray, A.S., Marten, R., Johnson, A. & Martin, P., 1987: Analysis for naturally occuring radionuclides at environmental concentrations by gamma spectrometry. *Journal of Radioanalytical and Nuclear Chemistry Articles 115,* 263–288.

Murray, A.S. & Wintle, A.G., 2000: Luminescence dating of quartz using an improved single-aliquot regenerative-dose protocol. *Radiation Measurements 32,* 57–73.

Murray, A.S. & Wintle, A.G., 2003: The single aliquot regenerative dose protocol: potential for improvements in reliability. *Radiation Measurements 37,* 377–381.

Nenonen, K., Vanne, J. & Laaksonen, H., 2010: Laserkeilaus – uusi menetelmä geologiseen kartoitukseen ja tutkimukseen [Airborne laser scanning – a new method to geological mapping and research]. *Geologi 62,* 62–69.

Palmu, J.-P. & Nenonen, K., 2015: Maaston laserkeilausaineistot maa- ja kallioperän korkokuvan ja rakenteiden heijastajana. Summary: Terrain models produced by LIDAR scanning reflect the relief and structure of the bedrock and Quaternary overburden. *Geologi 67,* 18–25.

Prescott, J.R. & Hutton, J.T., 1994: Cosmic ray contributions to dose rates for luminescence and ESR dating: large depths and long-term time variations. *Radiation Measurements 23,* 497–500.

Räisänen, J., 2014: Sodankylän alueen maaperäkartoitus 2013–2014 (Väliraportti). Geological Survey of Finland, Archive Report 52/2014, 22 p. (in Finnish).

Salonen, V.-P., Kaakinen, A., Kultti, S., Miettinen, A., Eskola, K.O. & Lunkka, J.P., 2008: Middle Weichselian glacial event in the central part of the Scandinavian Ice Sheet recorded in the Hitura pit, Ostrobothnia, Finland. *Boreas 37,* 38–54.

Salonen, V.-P., Moreau, J., Hyttinen, O. & Eskola, K.O., 2014: Mid-Weichselian interstadial in Kolari, western Finnish Lapland. *Boreas 43*, 627–638. doi: http://dx.doi.org/10.1111/bor.12060.

Sarala, P., 2012: How long the glaciations do lasted during Weichselian in Finland? *In* Þ. Sæmundsson & Í.Ö. Benediktsson (eds.): Programme and Abstracts, 30th Nordic Geological Winter Meeting, Reykjavik, Iceland, 9–12 January, 60. Geoscience Society of Iceland, Reykjavik.

Sarala, P. & Eskola, T., 2011: Middle Weichselian Interstadial deposit in Petäjäselkä, Northern Finland. *E&G – Quaternary Science Journal 60*, 488–492.

Sarala, P.O., Johansson, P.W., Jungner, H. & Eskola, K.O., 2005: The Middle Weichselian interstadial: new OSL dates from southwestern Finnish Lapland. *In* V. Kolka & O. Korsakova (eds.): *Quaternary geology and landforming pro-*

cesses: proceedings of the international field symposium, Kola Peninsula, NW Russia, September 4–9, 56–58. Kola Science Centre RAS, Apatity.
Sarala, P. & Ojala, V.J., 2008: Implications of complex glacial deposits for till geochemical explora-tion: Examples from the central Fennoscandian ice sheet. *In* Ó. Stefánsson (ed.): *Geochemistry Research Advances*, Chapter 1, 1–29. Nova, New York, NY.
Sarala, P., Pihlaja, J., Putkinen, N. & Murray, A., 2010: Composition and origin of the Middle Weichselian interstadial deposit in Veskoniemi, northern Finland. *Estonian Journal of Earth Sciences 59*, 117–124. doi: http://dx.doi.org/10.3176/earth.2010.2.
Smith, C.A. & Peterson, G., 2014: Quaternary geomorphology of the Siljan area, central Sweden. *Journal of Maps 10*, 521–528.
Smith, C.A., Sundh, M. & Mikko, H., 2014: Surficial geology indicates early Holocene faulting and seismicity, central Sweden. *International Journal of Earth Sciences 103,* 1711–1724.
Sutinen, R., Hyvönen, E. & Kukkonen, I., 2014: LiDAR detection of paleolandslides in the vicinity of the Suasselkä posglacial fault, Finnish Lapland. *International Journal of Applied Earth Observation and Geoinformation 27,* 91–99.
Tabor, R.W., Haeussler, P.J., Haugerud, R.A. & Wells, R.E., 2011: Lidar-Revised Geologic Map of the Uncas 7.5' Quadrangle, Clallam and Jefferson Counties, Washington. U.S. Geological Survey Scientific Investigations Map 3160, 25 p., scale 1:250,000. http://pubs.usgs.gov/sim/3160/.
Turney, C.S.M., Flannery, T.F., Roberts, R.G., Reid, C., Fifield, L.K., Higham, T.F.G., Jacobs, Z., Kemp, N., Colhoun, E.A., Kalin, R.M. & Ogle, N., 2008: Late-surviving megafauna in Tasmania, Australia, implicate human involvement in their extinction; *Proceedings of the National Academy of Sciences 105,* 12150–12153. doi:http://dx.doi.org/10.1073/pnas.0801360105.
Tyrväinen, A., 1984: *Kallioperäkarttojen selitykset, Lehdet 3713 ja 3714* [Explanation to the maps of pre-Quaternary rocks, Sheets 3713 and 3714]. Geological Survey of Finland, Espoo.
Väisänen, U., Maunu, M. & Kähkönen, A., 1989: Jänkävuopaja. Maps of Quaternary deposits 1:20 000, Map sheet 3713 08. Geological Survey of Finland.
Väisänen, U. & Maunu, M., 1990: Sodankylä. Maps of Quaternary deposits 1:20 000, Map sheet 3713 09. Geological Survey of Finland.
Väisänen U. & Maunu, M., 2004: Sattanen. Maps of Quaternary deposits 1:20 000, Map sheet 3714 07 with explanations. Geological Survey of Finland.
Webster, T.L., Murphy, J.B., Gosse, J.G. & Spooner, I., 2006: The application of lidar-derived digital elevation model analysis to geological mapping: an example from the Fundy Basin, Nova Scotia, Canada. *Canadian Journal of Remote Sensing 32*, 173–193.
Wilson T. & Csathó B., 2007: Airborne laser swath mapping of the Denton Hills, Transantarctic Mountains, Antarctica: Applications for structural and glacial geomorphic mapping. *In* A.K. Cooper & C.R. Raymond (eds.): *Antarctica: A Keystone in a Changing World – Online Proceedings of the 10th ISAES*. USGS Open-File Report 2007-1047, Short Research Paper 089, 6 p. doi: http://dx.doi.org/10.3133/of2007-1047.srp089.